

# The Role of Inner-Core Moisture in Tropical Cyclone Predictability and Practical Forecast Skill

KERRY EMANUEL

*Lorenz Center, Massachusetts Institute of Technology, Cambridge, Massachusetts*

FUQING ZHANG

*Department of Meteorology and Atmospheric Science, and Center for Advanced Data Assimilation and Predictability Techniques, The Pennsylvania State University, University Park, Pennsylvania*

(Manuscript received 10 January 2017, in final form 18 April 2017)

## ABSTRACT

Errors in tropical cyclone intensity forecasts are dominated by initial-condition errors out to at least a few days. Initialization errors are usually thought of in terms of position and intensity, but here it is shown that growth of intensity error is at least as sensitive to the specification of inner-core moisture as to that of the wind field. Implications of this finding for tropical cyclone observational strategies and for overall predictability of storm intensity are discussed.

## 1. Introduction

Prediction of tropical cyclone intensity remains a significant challenge, with little improvement in forecast skill over the past few decades (DeMaria et al. 2014). This lack of improvement has been attributed to a variety of factors, from inadequate observations of the atmosphere and upper ocean, to lack of ability to assimilate observations, to model errors, but in recent years there has been a concerted effort to improve intensity forecasts (Gall et al. 2013).


In a recently published paper (Emanuel and Zhang 2016), the authors attempted to quantify the intrinsic predictability of tropical cyclone intensity and to distinguish the various causes of loss of predictability, using a perfect model framework to isolate the intrinsic predictability. They showed that forecast intensity error out to a few days is dominated by errors in the initial wind field, after which errors in forecasting the large-scale environment begin to dominate through their effects on the track of and wind shear experienced by the storms. They also provided evidence that there remains a significant gap

between operational intensity forecast skill and skill that is theoretically achievable given optimistic estimates of tropical cyclone initial-condition specification and of large-scale environmental prediction skill.

In that work, the water vapor content of the inner core of the tropical cyclone model was held fixed between the control and perturbation experiments and so was not considered as a source of forecast error. Here we focus on the importance of the correct initialization of inner-core moisture.

Here we use the term “inner core” somewhat loosely to denote the broad region of ascent that includes the eyewall and weaker but deep convection just outside it but does not include the eye itself (if there is one) or the region of more isolated spiral bands farther away from the center. In idealized numerical simulations that begin with a weak cyclonic disturbance near the surface, storm-scale ascent occurs inside the radius at which the radial mass flux peaks, and this radius could be used, though not without some ambiguity, to separate the inner core from the outer region, while the eye could be identified with weak descent inside the eyewall.

---

 Denotes content that is immediately available upon publication as open access.

---

Corresponding author: Kerry Emanuel, emanuel@mit.edu



This article is licensed under a [Creative Commons Attribution 4.0 license](http://creativecommons.org/licenses/by/4.0/) (<http://creativecommons.org/licenses/by/4.0/>).

There are abundant reasons to focus on inner-core moisture. Emanuel (1989) demonstrated, using a simple balanced axisymmetric tropical cyclone model, that the inner core, defined as in the preceding paragraph, had to be nearly saturated before intensification by surface fluxes could begin. He showed that even small degrees of subsaturation resulted in convective downdrafts, driven by evaporation of rain, that import low-entropy air into the subcloud layer and thereby negate the tendency of surface fluxes to increase subcloud-layer entropy.

Moisture outside what we are here referring to as the inner core is also important to storm intensity, especially when environmental shear is present. If the shear is strong enough, lower moist static energy outside the core can be advected into the core in a process that is known as “ventilation” (Tang and Emanuel 2010). But this happens on an advective time scale, so moisture anomalies far from the storm center take some time to influence the core, whereas initial errors in inner-core moisture have an almost immediate effect. While we here focus on inner-core moisture anomalies, we do not claim that anomalies outside the core are unimportant, particularly at longer lead times.

Rappin et al. (2010) used the Weather Research and Forecasting (WRF) Model to perform three-dimensional simulations of tropical cyclogenesis at high (convection permitting) horizontal resolution. They also demonstrated that surface intensification of vortices begins only if and when a mesoscale column in the storm’s core becomes nearly saturated. Before that happens, or in failed cases of genesis, convective downdrafts quench any tendency of enhanced surface enthalpy fluxes to increase boundary layer entropy, even though a mesocyclone aloft may intensify by evaporation and melting of falling precipitation.

More fundamentally, Pauluis and Held (2002) showed that, in ordinary radiative–convective equilibrium, the overall irreversible entropy production in the system is limited by the radiative export of entropy to space and that the great majority of this limited total entropy production is used up in mixing (diffusion) across strong gradients of water vapor, leaving very little for kinetic energy dissipation. To transition to a state having large dissipation of kinetic energy, as with tropical cyclones, there must be a drastic reduction in entropy production by mixing across water vapor gradients. This can only happen if the moist convection takes place in nearly saturated air so that there is little mixing of dry air into clouds.

Even when a tropical cyclone does develop, it remains susceptible to mixing of dry air into the core, as first suggested by Simpson and Riehl (1958). Tang and Emanuel (2010) showed quantitatively how ventilation of the tropical cyclone core reduces the storm’s intensity and that too

much ventilation will destroy it altogether. This is consistent with Pauluis and Held’s (2002) observation that entropy production is easily dominated by mixing of dry and moist air, subtracting from that which could be used for kinetic energy dissipation.

It stands to reason, therefore, that the rate of intensification of tropical cyclones is sensitive to the degree of subsaturation of the inner core, where the eyewall convection occurs. In the simple Coupled Hurricane Intensity Prediction System (CHIPS; Emanuel et al. 2004), used routinely to predict tropical cyclone intensity in near–real time,<sup>1</sup> the inner-core moisture is initialized by matching the initial rate of intensity change to the observed change of intensity over the history of the storm to date. Failure to initialize the inner-core moisture properly yields large forecast errors, even if the initial maximum wind speed is free of error.

Our purpose here is to quantitatively assess the influence of initial inner-core moisture errors on tropical cyclone prediction skill. We take three approaches to this. First, we examine a single case study: Hurricane Joaquin of 2015. Using a full-physics WRF Model (Skamarock et al. 2008) and an ensemble-based data assimilation system (Zhang et al. 2009; Weng and Zhang 2012, 2016), we produce several large ensembles of forecasts that differ in their initialization of inner-core moisture either with or without initial differences in wind speed, while keeping the environmental initial conditions and boundary conditions the same for all ensemble members. We repeat this exercise using the simple CHIPS model. Second, we extend the work of Emanuel and Zhang (2016) to include initial inner-core moisture perturbations, comparing their growth to the growth of error from other sources in a perfect model framework. Finally, we introduce a new toy intensity model, consisting of a pair of ordinary differential equations, designed to mimic the behavior of the full CHIPS model, and use this to assess error growth in a simple forecast system.

## 2. Sensitivity to inner-core moisture: A case study

We begin with a single case as an example of the sensitivity of intensity forecasts to initial inner-core moisture. The case in point is Atlantic Hurricane Joaquin of 2015. Joaquin developed east of the Bahamas on or about 27 September and drifted slowly southwestward, turning back northeastward on 2 October. It intensified very rapidly, beginning at about 1200 UTC 29 September, a development that the National Hurricane Center forecast and most objective guidance products failed to anticipate,

<sup>1</sup> <http://wind.mit.edu/~emanuel/storm.html>.

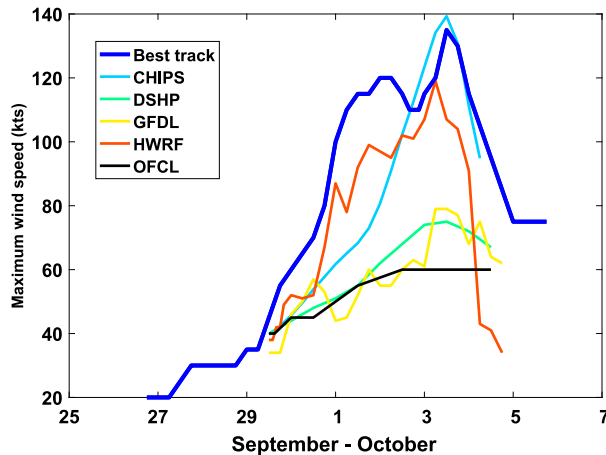


FIG. 1. Evolution over time of the maximum surface wind speed in Hurricane Joaquin as observed (thick blue) and predicted at 1200 UTC 29 Sep according to the official National Hurricane Center forecast (OFCL; black), and four objective intensity guidance products: CHIPS (light blue), the Decay Statistical Hurricane Prediction (DSHP; green), the Geophysical Fluid Dynamics Laboratory model (GFDL; yellow), and the Hurricane Weather Research and Forecasting Model (HWRF; red).

as shown in Fig. 1. More remarkable is the large spread in forecast intensities. At 1200 UTC 3 October, when the storm reached its peak intensity of 135 knots ( $1 \text{ kt} = 0.51 \text{ m s}^{-1}$ ), forecast intensities ranged from 60 to 140 kt. This is a good example of the large uncertainty and low skill currently associated with tropical cyclone intensity forecasts. Tragically, in this case, failure to anticipate the rapid development and high intensity achieved by Joaquin may have been among the factors leading to the loss of the ship *El Faro* with all hands.

#### a. WRF Model simulations

The ensemble forecasts based on the WRF Model, version 3.5.1 (Skamarock et al. 2008), initiated with the ensemble Kalman filter (EnKF) analysis perturbations at 1200 UTC 29 September 2015 from The Pennsylvania State University (PSU) experimental real-time convection-permitting hurricane analysis and forecast system produced a large ensemble spread, consistent with the large errors in Joaquin's intensity forecasts, as well as the large divergence in forecast intensity guidance (Fig. 1) and among the ensemble track forecasts (not shown). The real-time PSU WRF-EnKF system (Weng and Zhang 2016) used a 60-member ensemble with a finest grid spacing of 3 km that assimilated nonradiance conventional observations plus reconnaissance airborne dropsonde and flight-level observations for Joaquin.

To separate the influence of the inner-core versus environmental conditions on Joaquin's intensity forecast uncertainties, we performed a WRF-based ensemble

forecast experiment that is similar to the real-time PSU WRF-EnKF ensemble, but using only the real-time ensemble perturbations in the inner-core region (within a radius of 300 km) while relocating the center of each member's initial vortex to the PSU WRF-EnKF analysis mean position. The environmental conditions (outside a radius of 600 km from the vortex) are the same in all members and are interpolated from the NCEP operational Global Forecast System (GFS) analysis. Linear interpolation is applied to each member for radii between 300 and 600 km, assigning a decreasing weight (from 1 to 0) to the real-time WRF-EnKF initial ensemble perturbations and an increasing weight (from 0 to 1) to the GFS analysis. The mean and ensemble spread (in terms of standard derivation) of the azimuthally averaged tangential wind and relative humidity are shown in Fig. 2. The spread in surface azimuthal wind reaches peak values of about  $10 \text{ m s}^{-1}$ , while the relative humidity spread reaches a peak amplitude of around 16% near the storm center in the middle to upper troposphere. But note that the largest humidity perturbations are in the unsaturated eye region and probably do not have much effect on subsequent intensification. We will address this issue presently.

This new WRF ensemble simulation with only initial inner-core perturbations reproduced the intensity forecast uncertainties (Fig. 3), but as we used the same GFS environmental conditions for each ensemble member, there is little forecast divergence in the ensemble tracks (not shown), implying that, at least for this forecast initialization time of Joaquin, the track forecast is primarily influenced by the large-scale environment (to be examined in a separate study), while the intensity forecast is predominantly determined by the initial inner-core dynamic and thermodynamic conditions.

To isolate the influence of inner-core moisture above the hurricane boundary layer, we perform two other ensemble experiments, identical to that illustrated in Fig. 3, but with one retaining only moisture perturbations (Fig. 2, right) and the other retaining only moisture perturbations above the boundary layer (using a linear transition zone from zero perturbations at 900 hPa to full perturbations at 850 hPa) and outside of the eye (from zero perturbations at 25-km radius to full perturbations at 50 km). The results are shown in Figs. 4 and 5. These two additional ensemble experiments demonstrate that, while initial inner-core vortex intensity perturbations are strongly influential, there are considerable uncertainties in the hurricane intensity forecast with only inner-core moisture perturbations (Fig. 4). Moreover, even retaining the inner-core moisture perturbations only above the boundary layer and outside the eye will lead to considerable intensity spread (Fig. 5). Another ensemble experiment that is the same as

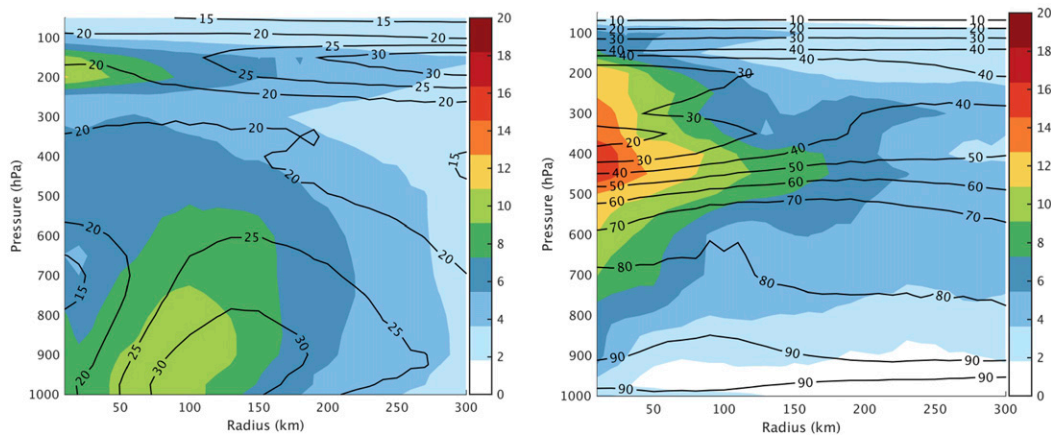


FIG. 2. Ensemble mean (solid black contours) and standard deviations (colored shading) of (left) azimuthally averaged tangential wind ( $\text{m s}^{-1}$ ) and (right) relative humidity (%) for the WRF Model simulations.

in Fig. 5, but retaining only the boundary layer moisture perturbations, shows a similar level of influence on hurricane intensity (not shown).

Sensitivity of tropical cyclone intensity to initial moisture uncertainties was also investigated through real-data, full-physics, convection-permitting ensemble simulations in Sippel and Zhang (2008, 2010), Zhang and Sippel (2009), and Munsell et al. (2013, 2015), though none of these previous studies exclusively focused on realistic inner-core moisture-only perturbations. Meanwhile, recently idealized full-physics WRF simulations (Zhang and Tao 2013; Tao and Zhang 2014) also showed that the intensity forecast can be intrinsically limited (especially during the development stage), even if only perturbed with minute, unobservable boundary layer moisture uncertainties for moderately sheared tropical cyclones, though a constant environmental condition will eventually grow the ensemble members to similar intensity after rapid intensification.

### b. CHIPS simulations

CHIPS (Emanuel et al. 2004) is a simple, axisymmetric, quasi-balanced tropical cyclone model phrased in angular momentum coordinates and coupled to a simple, one-dimensional upper-ocean model that allows for the physics of storm-induced vertical mixing. CHIPS has been used for about 15 years to make real-time forecasts of tropical cyclone intensity globally. The forecasts themselves have been archived, together with key environmental parameters along the forecast track; these include potential intensity and vertical shear of the large-scale horizontal wind. In recent years, we have run a seven-member ensemble defined by perturbing the initial intensity and inner-core moisture and predicted environmental wind shear. The control forecast for Joaquin made at 1200 UTC 29 September 2015 is shown in Fig. 1.

After a particular event has occurred, we routinely rerun the CHIPS model using the observed (rather than forecast) track and the operationally analyzed wind shear and potential intensity along the track. This allows us to minimize error sources related to incorrectly forecast track and wind shear so as to focus on model and initialization errors.

Here we create ensembles of such poststorm simulations by perturbing the initial intensity and inner-core moisture. Each ensemble member uses the same track and large-scale environmental conditions. The initial vortex is specified by a peak gradient wind at the surface, and the radius at which this gradient wind reaches its peak value. Thus, perturbing the initial peak wind is straightforward.

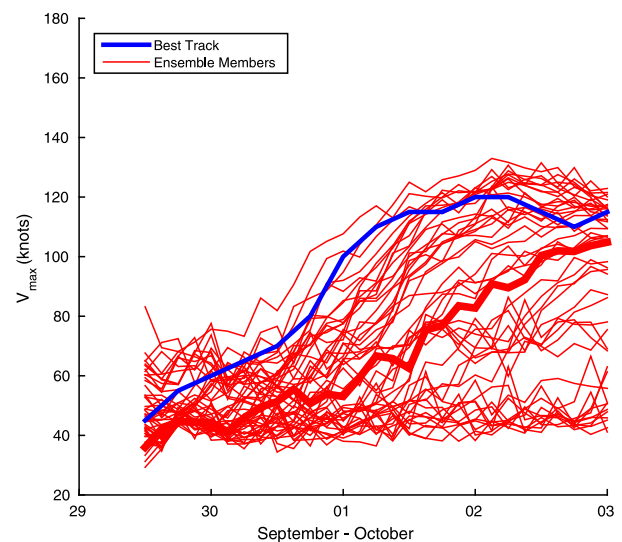


FIG. 3. The intensity forecast of the WRF ensemble using only the PSU WRF-EnKF real-time ensemble analysis perturbations in the inner-core region. The thick red line shows the ensemble member considered to be of highest quality whose initial conditions and first 48-h forecast match closely to the best-track observations.

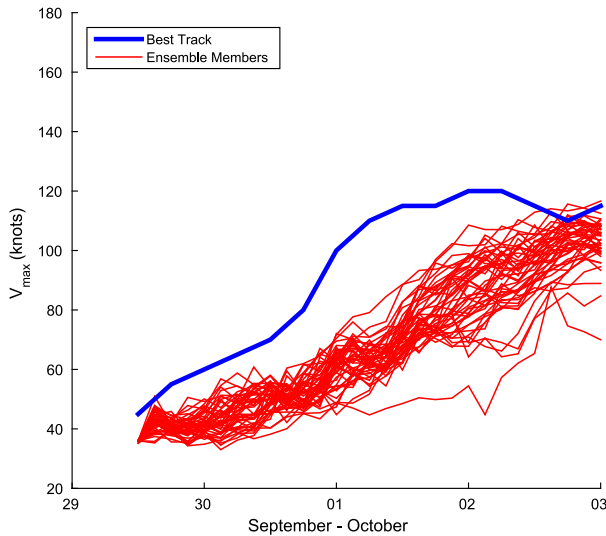


FIG. 4. As in Fig. 3, but retaining only the inner-core moisture perturbations. The initial wind speed corresponds to PSU WRF-EnKF real-time analysis mean shown in Fig. 2 (left).

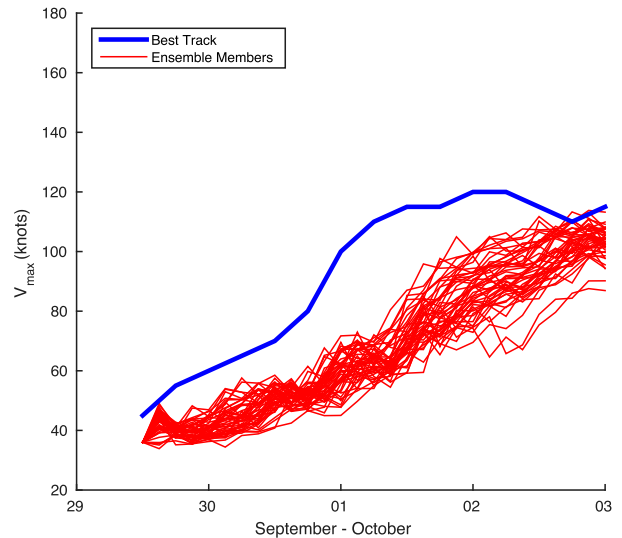


FIG. 5. As in Fig. 4, but using only initial inner-core moisture perturbations above the boundary layer (with a linear transition zone from zero perturbations at 900 hPa to full perturbations at 850 hPa) outside of the eye (from zero perturbations at 25-km radius to perturbations at 50 km). The initial wind speed corresponds to PSU WRF-EnKF real-time analysis mean shown in Fig. 2 (left).

For real-time forecasts, CHIPS is run from the inception of the storm up to the current time, and the degree of inner-core saturation is continuously varied so as to best match the history of the storm’s intensity. In these forecasts, and in what follows, “inner core” is defined to be within 1.3 times the radius of maximum winds. The rate of intensification of CHIPS-simulated storms is quite sensitive to inner-core moisture, so matching the simulated storm’s intensity to the history of the real storm’s intensity up to the current time has the effect of initializing the inner-core moisture. This is highly advantageous in view of the paucity of observations of tropospheric water vapor in the inner cores of tropical cyclones. We shall return to this point in advocating for tropical cyclone data assimilation that accounts for at least the recent history of the storm.

Once initialized, the inner-core moisture is predicted by a rate equation that accounts for vertical advection within the storm and a parameterized interaction with environmental wind shear. [See Emanuel et al. (2004) for a more complete discussion of this.]

For the present purposes, we initialize the inner-core moisture through specification of a parameter we label  $d$ , which varies from 0 to 1. When  $d = 0$ , the initial inner-core moist static energy at midlevels in the troposphere is identical to that of the unperturbed environment, while  $d = 1$  corresponds to saturation of the inner core. Thus,  $d$  is defined as

$$d \equiv \frac{h_{ic} - h_e}{h_{ic}^* - h_e},$$

where  $h_{ic}$  is the moist static energy of the inner core,  $h_{ic}^*$  is its saturation value, and  $h_e$  is the environmental moist static energy.

Figure 6a shows the evolution of 21 CHIPS hindcasts in which the initial value of the  $d$  parameter is fixed at 0.9 while the initial wind speed is varied over the range from  $-5$  to  $+5 \text{ m s}^{-1}$  in increments of  $0.5 \text{ m s}^{-1}$ . This range is conservative relative to contemporary estimates of uncertainty in tropical cyclone intensity (Landsea and Franklin 2013). Clearly, the forecast intensity is sensitive to the initial intensity, which is consistent with the full 3D convection-permitting WRF ensemble experiments shown in Fig. 2 for the same event.

All of the hindcasts shown in Fig. 6b are initialized at the observed intensity, but with initial  $d$  values ranging from 0.5 to 1 in increments of 0.05. (If the environmental relative humidity were 50%, an initial  $d$  value of 0.5 would correspond to an inner-core relative humidity of about 75%. In this case, varying  $d$  values ranging from 0.5 to 1 would correspond to varying the relative humidity over a range of about 25%. This is a bit larger than the ensemble variance we used in the WRF simulations (Fig. 2). To our knowledge there are no published studies of the uncertainty in initial estimates of observed tropical cyclone inner-core humidity.) The intensity evolution is quite sensitive to inner-core moisture variations over a realistic range. Thus, the CHIPS model exhibits roughly the same sensitivity to initial inner-core moisture as exhibited by the full WRF

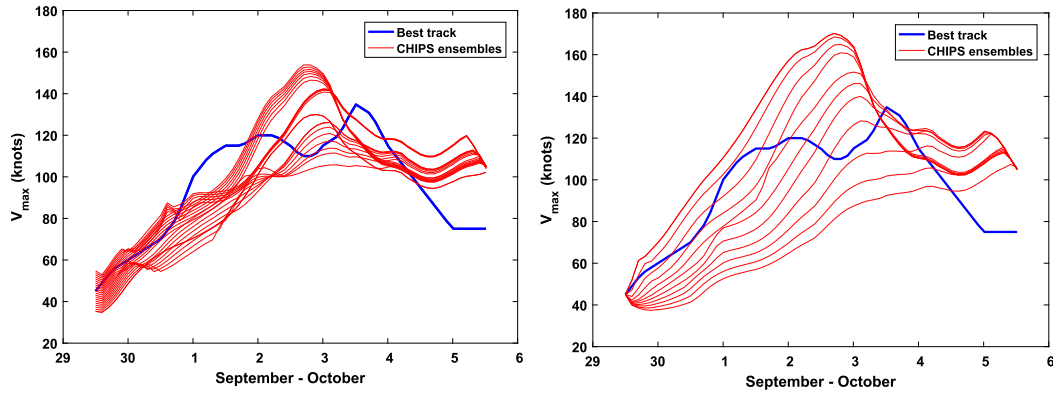


FIG. 6. Evolution of CHIPS hindcasts (red) of Joaquin, initialized at 1200 UTC 29 Sep 2015, compared to best-track intensity (blue). (a) Each hindcast is initialized with  $d = 0.9$  and with the initial wind speed varying by  $\pm 5 \text{ m s}^{-1}$  from the initial best-track value. (b) Each hindcast is initialized with the observed wind speed, but with  $d$  values ranging from 0.5 to 1.

Model ensemble experiments discussed in the previous subsection (Figs. 4, 5).

This sensitivity, so far demonstrated across two models, is the main result of the present work.

### c. Tropical cyclone intensity simulator

Partly to encourage further tropical cyclone intensity predictability studies, we developed a highly simplified tropical cyclone intensity algorithm that can be very rapidly coded and solved. We started with a theoretical development equation developed by Emanuel (2012) for the special case in which a tropical cyclone has a completely saturated inner core and develops without interaction with shear or feedback from the ocean or from isothermal expansion effects:

$$\frac{dV}{dt} \cong \frac{C_D}{2h} (V_p^2 - V^2), \quad (1)$$

where  $V$  is the maximum circular wind speed near the surface,  $C_D$  is the surface drag coefficient,  $h$  is a boundary layer depth, and  $V_p$  is the potential intensity modified by a function of the surface exchange coefficients of enthalpy and momentum. We sought to modify (1) to account for unsaturated inner cores, wind shear, and interaction with the underlying ocean. After much experimentation, we developed the following pair of ordinary differential equations:

$$\frac{dV}{dt} = \frac{1}{2} \frac{C_D}{h} (\alpha V_p^2 m^3 - V^2), \quad (2)$$

and

$$\frac{dm}{dt} = \frac{1}{2} \frac{C_D}{h} [(1 - m)V - 2.2Sm], \quad (3)$$

where  $V$  is the maximum circular wind speed,  $m$  is an inner-core moisture variable that varies between 0 and 1,  $S$  is the magnitude of the 850–250-hPa environmental wind shear, and  $\alpha$  is an ocean interaction parameter. [In (2) and (3), the units of  $V$ ,  $V_p$ ,  $S$ , and  $h$  must be consistent.] The ocean feedback parameter is modeled after the results of Schade and Emanuel (1999):

$$\alpha = 1 - 0.87e^{-z}, \quad (4)$$

where

$$z \equiv 0.01\Gamma^{-0.4} h_m u_T V_p V^{-1}. \quad (5)$$

Here,  $\Gamma$  is the submixed-layer thermal stratification [ $\text{K} (100 \text{ m})^{-1}$ ],  $h_m$  is the ocean mixed-layer depth (m), and  $u_T$  is the storm translation speed ( $\text{m s}^{-1}$ ).

In (2) and (3) we have not explicitly accounted for isothermal expansion effects, though they may be incorporated in the definition of  $V_p$ .

Note that, in the absence of ocean feedback ( $\alpha = 1$ ) and shear, the steady solution of (2) and (3) is  $V = V_p$ ,  $m = 1$ , as expected. If we regard the product  $2.2Sm$  as the ventilation  $v$  introduced by Tang and Emanuel (2010), then, in the absence of ocean feedback, the steady solution of (2) and (3) is given as the solution to

$$V^{*5/3} - V^* + v^* = 0, \quad (6)$$

where the asterisks indicate that the quantity has been normalized by the potential intensity  $V_p$ . This may be compared to the equilibrium equation developed by Tang and Emanuel (2010), which has the form

$$V^{*3} - V^* + v^* = 0. \quad (7)$$

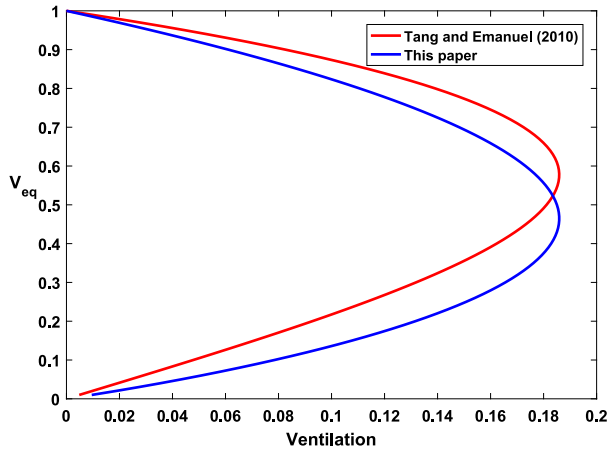


FIG. 7. Equilibrium solutions for normalized maximum wind as a function of normalized ventilation, for Tang and Emanuel (2010; red), and of (6) (blue). The upper branches are stable equilibria, while the lower branches are unstable.

The different exponents in (6) and (7) arise from different assumptions about the physics and from the desire here to closely mimic the full CHIPS model behavior. Solutions to (6) and (7), normalized to have the same threshold value of  $v^*$ , are compared in Fig. 7. They are quite similar in form. As shown by Tang and Emanuel (2010), the upper branches of the solution are stable equilibria, while the lower branches are unstable.

In our case (and perhaps in that of Tang and Emanuel 2010),  $v^*$  depends on  $m$ , so the solutions to (6) are not truly in terms of external quantities. Expressed as a function of the external quantity  $S^*$  (shear normalized by potential intensity), the equilibrium equation is

$$V^{*1/3} - V^* - S^* = 0. \tag{8}$$

Solutions of (8) are plotted in Fig. 8. Note that the upper stable equilibrium intensity decays almost linearly with increasing shear, until the shear approaches its critical value, when the intensity drops off more sharply. Also note that the critical intensity needed for amplification (the lower branch of the curve) is very small until the shear approaches its critical value. Above the critical shear, given by the rightmost point in Fig. 8, no equilibrium solution exists, and all solutions decay over time.

We apply the system given by (2) and (3) to the forecast of Joaquin initialized as before at 12 UTC 29 September 2015. As before, we drive the simple model with the analyzed potential intensity, environmental wind shear, and upper-ocean properties along the track. We use  $C_D = 1.2 \times 10^{-3}$  and  $h = 1400$  m and integrate the system with a simple leapfrog time scheme with an Asselin filter value of 0.1 and a time step of 240 s. A 6-day forecast with

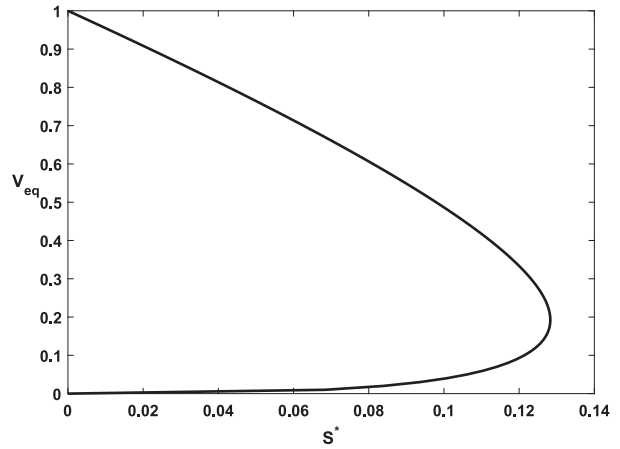


FIG. 8. Solution of (8) for the equilibrium maximum wind speed as a function of the normalized environmental wind shear  $S^*$ . As before, the upper branch is stable while the lower branch is unstable. The rightmost point of the curve represents a critical shear above which no equilibrium solution exists and all solutions decay with time.

this scheme runs in about 0.002 s on an ordinary laptop computer.

As before, we run one ensemble in which perturbations ranging from  $-5$  to  $+5 \text{ m s}^{-1}$  in increments of  $0.5 \text{ m s}^{-1}$  are added to the observed initial wind speed. For these simulations, we initialized  $m$  with a value of 0.3. In a second ensemble, we fix the initial intensity at its observed value while varying the initial value of  $m$  from 0.1 to 0.6 in increments of 0.05. The results of these two sets of simulations are shown in Fig. 9 together with the evolutions of the observed potential intensity and environmental wind shear along the observed track, the best-track intensity, and a single simulation of the full CHIPS model (one of the simulations displayed in Fig. 6).

Comparing these results with those of the full CHIPS model in Fig. 6, it is clear that the simple model intensity errors do not amplify as quickly (or decay as fast), perhaps because the nonlinearity of the simple model is weaker than that of the full CHIPS. But even in this simple model, errors resulting from the moisture initialization amplify quickly over the first day or so and persist for many days. But once the storm ceases intensifying, the errors collapse smoothly to zero as the storm equilibrates to environmental conditions. This error decay is also evident in the full CHIPS simulations (Fig. 6) but happens more slowly.

We hope that our simple system, consisting of (2)–(5), will inspire further studies of intrinsic tropical cyclone intensity predictability, and we believe it may serve as an alternative to purely statistical intensity algorithms for use in tropical cyclone risk models.

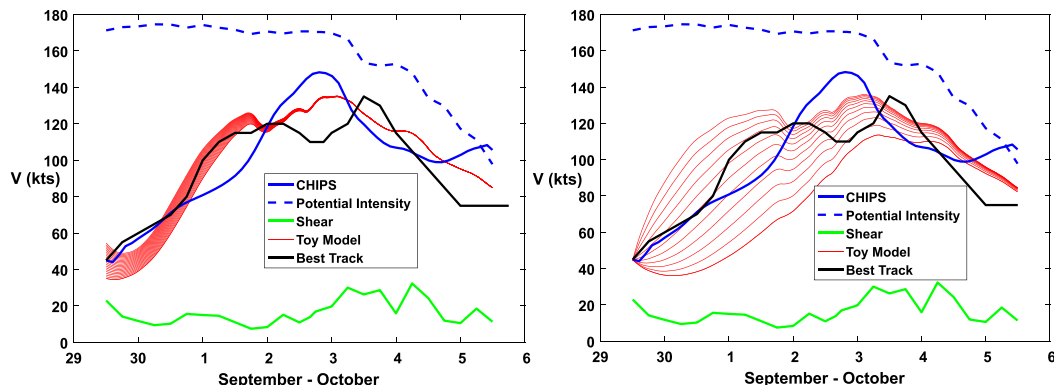


FIG. 9. Evolutions of ensembles of the simple model (red) initialized at 1200 UTC 29 Sep 2015, compared to the best-track intensity (black) and a single hindcast using the full CHIPS model (blue). Potential intensity (dashed blue) and environmental shear (green) are also shown. (left) An ensemble formed by varying the initial intensity by  $\pm 5 \text{ m s}^{-1}$ , with the initial value of  $m$  fixed at 0.3. (right) An ensemble initialized with the observed intensity, but with the initial value of  $m$  varying from 0.1 to 0.6.

### 3. Comparative effects of initial inner-core moisture on intensity errors

To explore more comprehensively the error growth owing to moisture initialization errors, we apply the framework developed by Emanuel and Zhang (2016). They used the tropical cyclone risk model of Emanuel et al. (2008) to simulate 3100 tropical cyclones in the North Atlantic, downscaled from NCAR–NCEP reanalyses. The storms were initialized with intensities varying randomly between 10 and 110 kt and run forward until their surface winds dropped below a threshold. The storms were then reinitialized with perturbations applied to their initial intensities and/or to their tracks and environmental wind shears. Comparison of these perturbed simulations to the control gave estimates of intensity error growth over time. [See Emanuel and Zhang (2016) for detailed descriptions of the experiments.]

All the events simulated in that work were initialized with the CHIPS moisture parameter  $d$  set to 1, so sensitivity to moisture initialization was not examined. Here we add one new set of simulations identical to the control set but with  $d = 0.8$  so each event begins with a drier inner core. (For an environmental relative humidity of 50%, this corresponds to an inner-core relative humidity of about 90%.) The root-mean-square difference between this set of simulations and the control is shown by the cyan curve in Fig. 10 and compared to the other error sources documented by Emanuel and Zhang (2016). (Figure 10 is identical to their Fig. 4, but with the addition of the cyan curve showing error growth due to initial inner-core moisture perturbations.)

Consistent with our analyses of the Joaquin simulations, error growth owing to initial inner-core moisture

errors is very fast and reaches a limit very quickly. For the perturbation to the CHIPS  $d$  parameter used here, this limiting error is somewhat larger than that resulting from the initial intensity perturbations used by Emanuel and Zhang (2016). The initial inner-core humidity perturbation is equivalent to 20% of the difference between the actual and saturation specific humidities on the middle troposphere, yet this is sufficient to cause rapid divergence of the solution from the control.

This result generalizes our findings from the single case study of Hurricane Joaquin: failure to properly initialize

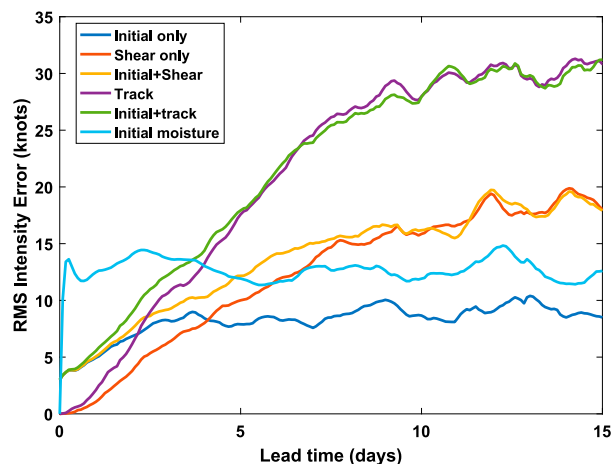


FIG. 10. As in Fig. 4 from Emanuel and Zhang (2016), but with the addition of root-mean-square intensity error owing solely to initial inner-core moisture perturbations (cyan curve). Other curves are errors resulting from initial intensity error only (dark blue), errors in forecast environmental shear (red), initial intensity and forecast shear together (yellow), forecast track errors (magenta), and initial intensity and forecast track error together (green).



inner-core water vapor in the free troposphere can be a large source of tropical cyclone intensity error.

#### 4. Summary

Using the full-physics convection-permitting tropical cyclone data assimilation and forecast system developed by Zhang et al. (2009) and refined by Weng and Zhang (2016), we showed that the evolution of forecast intensity is sensitive to initial inner-core tropospheric moisture as well as to the initial wind field. This sensitivity is also apparent in the simpler CHIPS model (Emanuel et al. 2004) as well as a very simple intensity simulator presented here for the first time. For reasonable estimates of its magnitude, initial inner-core moisture error may well dominate forecast intensity error out to several days' lead time. Beyond that, errors in free-tropospheric moisture outside the core, though not examined here, also play a role, as they affect the magnitude of ventilation of the core if large-scale shear is present.

Sensitivity to initial inner-core moisture has been demonstrated in several previous modeling studies and is consistent with the finding by Pauluis and Held (2002) that irreversible entropy production in tropical convecting systems is dominated by irreversible mixing across strong moisture gradients. This dominance persists unless or until the convection penetrates air that is already saturated or very nearly so, thus reducing entropy production by mixing across water vapor gradients. Only then can entropy production by dissipation of the kinetic energy of wind become an important entropy source.

The sensitivity of tropical cyclone intensification to inner-core moisture has obvious implications for initializing tropical cyclone intensity forecasts. Unfortunately, water vapor is among the least well-observed quantities in tropical cyclone cores, and the presence of deep convection and strong flows suggests that water vapor presents a significant sampling problem.

On the other hand, this very sensitivity to moisture presents a significant opportunity for data assimilation, since the time history of intensity, being strongly influenced by inner-core moisture, contains important information about the latter. Our crude initialization of the operational CHIPS model takes advantage of this fact by adjusting the initial core moisture to match the recently observed intensification rate. This suggests that assimilation in the time domain, such as four-dimensional variational (4D-Var) or cycling EnKF with flow-dependent background error covariance, may be critical to the quality of tropical cyclone forecast initialization, provided it implicitly or explicitly recognizes the correlation between intensification rates and inner-core humidity.

Our results suggest that excellent initialization of the instantaneous wind and associated thermal fields cannot by themselves yield accurate intensity forecasts absent a high-quality initialization of tropospheric water vapor, at least in the storm's inner core. Unlike with temperature and wind, there is no instantaneous balance condition that constrains water vapor unless the air is completely saturated. Thus, improvement in tropical cyclone intensity forecasts will depend in part on better observations of inner-core water vapor and/or data assimilation schemes that are able to link inner-core moisture to observed rates of intensification.

*Acknowledgments.* The first author gratefully acknowledges support from ONR through Grant N000141410062. The second author is partially supported by ONR Grant N000140910526 and NOAA under the Hurricane Forecast Improvement Program (HFIP). The authors thank Yonghui Weng and Robert Nystrom for their help on the WRF experiments. Computing was conducted at the Texas Advanced Computing Center.

#### REFERENCES

- DeMaria, M., C. R. Sampson, J. A. Knaff, and K. D. Musgrave, 2014: Is tropical cyclone intensity guidance improving? *Bull. Amer. Meteor. Soc.*, **95**, 387–398, doi:10.1175/BAMS-D-12-00240.1.
- Emanuel, K., 1989: The finite-amplitude nature of tropical cyclogenesis. *J. Atmos. Sci.*, **46**, 3431–3456, doi:10.1175/1520-0469(1989)046<3431:TFANOT>2.0.CO;2.
- , 2012: Self-stratification of tropical cyclone outflow. Part II: Implications for storm intensification. *J. Atmos. Sci.*, **69**, 988–996, doi:10.1175/JAS-D-11-0177.1.
- , and F. Zhang, 2016: On the predictability and error sources of tropical cyclone intensity forecasts. *J. Atmos. Sci.*, **73**, 3739–3747, doi:10.1175/JAS-D-16-0100.1.
- , C. DesAutels, C. Holloway, and R. Korty, 2004: Environmental control of tropical cyclone intensity. *J. Atmos. Sci.*, **61**, 843–858, doi:10.1175/1520-0469(2004)061<0843:ECOTCI>2.0.CO;2.
- , R. Sundararajan, and J. Williams, 2008: Hurricanes and global warming: Results from downscaling IPCC AR4 simulations. *Bull. Amer. Meteor. Soc.*, **89**, 347–367, doi:10.1175/BAMS-89-3-347.
- Gall, R., J. Franklin, F. Marks, E. N. Rappaport, and F. Toepfer, 2013: The hurricane forecast improvement project. *Bull. Amer. Meteor. Soc.*, **94**, 329–343, doi:10.1175/BAMS-D-12-00071.1.
- Landsea, C. W., and J. L. Franklin, 2013: Atlantic hurricane database uncertainty and presentation of a new database format. *Mon. Wea. Rev.*, **141**, 3576–3592, doi:10.1175/MWR-D-12-00254.1.
- Munsell, E. B., F. Zhang, and D. P. Stern, 2013: Predictability and dynamics of a non-intensifying tropical storm: Erika (2009). *J. Atmos. Sci.*, **70**, 2505–2524, doi:10.1175/JAS-D-12-0243.1.
- , J. A. Sippel, S. A. Braun, Y. Weng, and F. Zhang, 2015: Dynamics and predictability of Hurricane Nadine (2012) evaluated through convection-permitting ensemble analysis and forecasts. *Mon. Wea. Rev.*, **143**, 4513–4532, doi:10.1175/MWR-D-14-00358.1.

- Pauluis, O., and I. M. Held, 2002: Entropy budget of an atmosphere in radiative–convective equilibrium. Part I: Maximum work and frictional dissipation. *J. Atmos. Sci.*, **59**, 125–139, doi:[10.1175/1520-0469\(2002\)059<0125:EBOAAI>2.0.CO;2](https://doi.org/10.1175/1520-0469(2002)059<0125:EBOAAI>2.0.CO;2).
- Rappin, E. D., D. S. Nolan, and K. Emanuel, 2010: Thermodynamic control of tropical cyclogenesis in environments of radiative–convective equilibrium with shear. *Quart. J. Roy. Meteor. Soc.*, **136**, 1954–1971, doi:[10.1002/qj.706](https://doi.org/10.1002/qj.706).
- Schade, L. R., and K. A. Emanuel, 1999: The ocean’s effect on the intensity of tropical cyclones: Results from a simple coupled atmosphere–ocean model. *J. Atmos. Sci.*, **56**, 642–651, doi:[10.1175/1520-0469\(1999\)056<0642:TOSEOT>2.0.CO;2](https://doi.org/10.1175/1520-0469(1999)056<0642:TOSEOT>2.0.CO;2).
- Simpson, R. H., and H. Riehl, 1958: Mid-tropospheric ventilation as a constraint on hurricane development and maintenance. Preprints, *Tech. Conf. on Hurricanes*, Miami Beach, FL, Amer. Meteor. Soc., D4-1–D4-10.
- Sippel, J. A., and F. Zhang, 2008: A probabilistic analysis of the dynamics and predictability of tropical cyclogenesis. *J. Atmos. Sci.*, **65**, 3440–3459, doi:[10.1175/2008JAS2597.1](https://doi.org/10.1175/2008JAS2597.1).
- , and —, 2010: Factors affecting the predictability of Hurricane Humberto (2007). *J. Atmos. Sci.*, **67**, 1759–1778, doi:[10.1175/2010JAS3172.1](https://doi.org/10.1175/2010JAS3172.1).
- Skamarock, W. C., and Coauthors, 2008: A description of the Advanced Research WRF version 3. NCAR Tech. Note NCAR/TN-475+STR, 113 pp., doi:[10.5065/D68S4MVH](https://doi.org/10.5065/D68S4MVH).
- Tang, B., and K. Emanuel, 2010: Midlevel ventilation’s constraint on tropical cyclone intensity. *J. Atmos. Sci.*, **67**, 1817–1830, doi:[10.1175/2010JAS3318.1](https://doi.org/10.1175/2010JAS3318.1).
- Tao, D., and F. Zhang, 2014: Effect of environmental shear, sea-surface temperature, and ambient moisture on the formation and predictability of tropical cyclones: An ensemble-mean perspective. *J. Adv. Model. Earth Syst.*, **6**, 384–404, doi:[10.1002/2014MS000314](https://doi.org/10.1002/2014MS000314).
- Weng, Y., and F. Zhang, 2012: Assimilating airborne Doppler radar observations with an ensemble Kalman filter for convection-permitting hurricane initialization and prediction: Katrina (2005). *Mon. Wea. Rev.*, **140**, 841–859, doi:[10.1175/2011MWR3602.1](https://doi.org/10.1175/2011MWR3602.1).
- , and —, 2016: Advances in convection-permitting tropical cyclone analysis and prediction through EnKF assimilation of reconnaissance aircraft observations. *J. Meteor. Soc. Japan*, **94**, 345–358, doi:[10.2151/jmsj.2016-018](https://doi.org/10.2151/jmsj.2016-018).
- Zhang, F., and J. A. Sippel, 2009: Effects of moist convection on hurricane predictability. *J. Atmos. Sci.*, **66**, 1944–1961, doi:[10.1175/2009JAS2824.1](https://doi.org/10.1175/2009JAS2824.1).
- , and D. Tao, 2013: Effects of vertical wind shear on the predictability of tropical cyclones. *J. Atmos. Sci.*, **70**, 975–983, doi:[10.1175/JAS-D-12-0133.1](https://doi.org/10.1175/JAS-D-12-0133.1).
- , Y. Weng, J. A. Sippel, Z. Meng, and C. H. Bishop, 2009: Cloud-resolving hurricane initialization and prediction through assimilation of Doppler radar observations with an ensemble Kalman filter: Humberto (2007). *Mon. Wea. Rev.*, **137**, 2105–2125, doi:[10.1175/2009MWR2645.1](https://doi.org/10.1175/2009MWR2645.1).